Endocrine (2020) 68:489–501
https://doi.org/10.1007/s12020-020-02242-3

REVIEW

Diagnosis and Management of pituitary disease with focus on the role of Magnetic Resonance Imaging

Amit Mahajan[1] · Richard A. Bronen[1] · Ali Y. Mian[2] · Sacit Bulent Omay[3] · Dennis D. Spencer[3] · Silvio E. Inzucchi[4]

Received: 17 October 2019 / Accepted: 24 February 2020 / Published online: 11 March 2020

Abstract
Magnetic resonance (MR) imaging is an essential tool in the diagnosis and management of pituitary diseases, indispensable for making correct treatment decisions. Successful management and follow-up of pituitary pathology requires an understanding of the MR appearance of normal and abnormal structures in the sellar region. This review will describe the MR appearance of the normal and abnormal pituitary gland and proposes an algorithm for the management strategy of some of the most common abnormalities in or around the sella.

Keywords Pituitary · MRI · Treatment/Management

Introduction

Magnetic resonance (MR) imaging is a powerful tool in the diagnosis and management of pituitary diseases and remains a critical diagnostic step in the initial assessment and differential diagnosis of sellar and parasellar masses. After the initial detection of such a mass, MR assessment of stability, growth or treatment response over time is indispensable to making correct treatment decisions. Successful management and follow-up of pituitary pathology requires an understanding of the MR appearance of normal and abnormal structures in the sellar region. This review will describe the appearance of the normal pituitary gland, its relationship to nearby structures and imaging appearances of some of the common sellar abnormalities. We then proceed to review key clinical and pathological issues related to the most common imaging abnormality of this area, namely pituitary tumors and propose a clinical management strategy for the most common types.

Normal anatomy of the sella

The normal pituitary gland consists of an anteriorly located adenohypophysis (including the pars distalis, pars intermedia and pars tuberalis) and the posterior pituitary (or neurohypophysis). The pars distalis constitutes the majority of the intrasellar adenohypophysis and secretes both glycoprotein and peptide hormones into the systemic circulation in response to stimulating hormones/factors released by the hypothalamus into the hypothalamic-pituitary portal venous plexus. The pars intermedia is considered vestigial in humans although it is known to secrete alpha-MSH. The pars tuberalis is an upward continuation of the pars distalis surrounding the central core of pituitary infundibulum and is a delicate layer of tissue permeated by the capillaries of the hypothalamic-pituitary portal plexus.

On MR imaging, the anterior pituitary is isointense to the cerebral gray matter on all imaging sequences. Intense, diffuse postcontrast enhancement of the pituitary gland (Fig. 1) and the pituitary infundibular stalk is noted within seconds of administration, reflecting its highly vascular nature as well as its location outside the blood-brain barrier. Most pathologies affecting the gland are recognized as hypo- or nonenhancing areas relative to normal enhancing gland. Dynamic contrast imaging following gadolinium administration is frequently used to

✉ Amit Mahajan
amit.mahajan@yale.edu

[1] Department of Radiology and Biomedical Imaging, Yale University School of Medicine, 333 Cedar St, CB-20, New Haven, CT 06520, USA

[2] Mallinckrodt Institute of Radiology, St. Louis, MO 63110, USA

[3] Department of Neurosurgery, Yale University School of Medicine, New Haven, CT, USA

[4] Section of Endocrinology, Department of Medicine, Yale University School of Medicine, New Haven, CT, USA

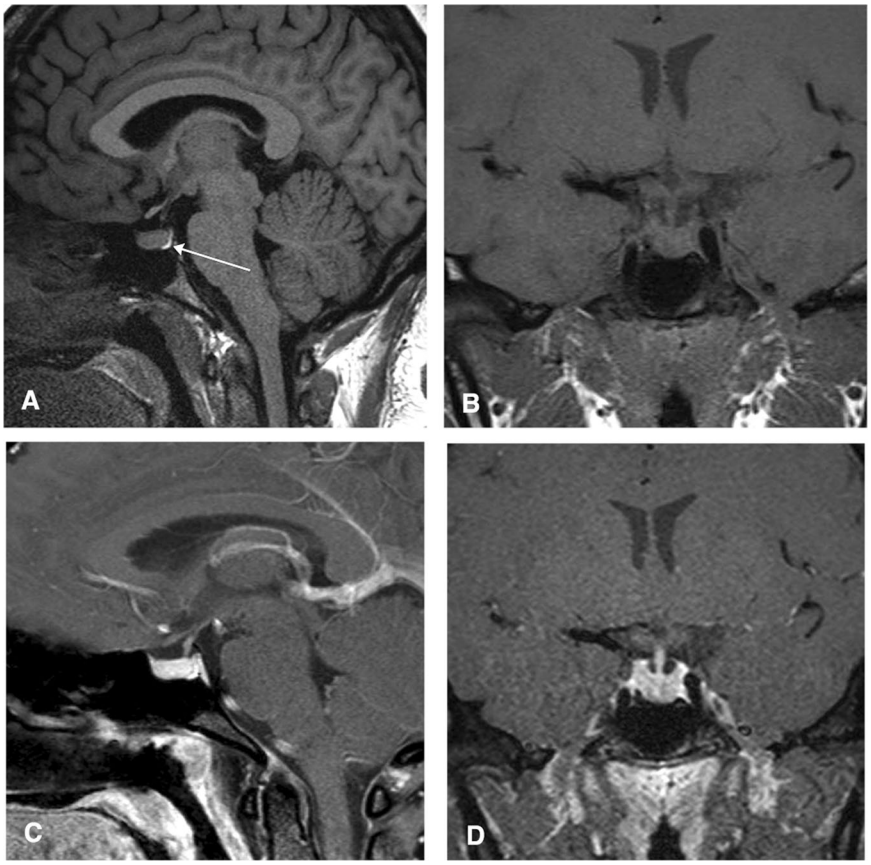

Fig. 1 Normal pituitary: Noncontrast T1-weighted sagittal (**a**) and coronal images (**b**) demonstrating a normal-sized anterior pituitary gland with hyperintense signal (arrow) within the normal posterior pituitary gland. Postcontrast sagittal (**c**) and coronal images (**d**) reveal diffuse enhancement of the infundibulum and the pituitary gland reflecting the lack of blood-brain barrier and hypervascularity of the pituitary gland and the infundibulum

evaluate for small adenomas and involves repeated, sequential imaging of the pituitary gland over a period of 1–5 min in order to optimally distinguish the tumor from the normal gland.

The pituitary gland demonstrates dynamic changes in size, shape and signal intensity during life, depending on the developmental and hormonal state of the individual. At birth, the gland is globular in shape, but becomes more flattened with age; height decreases while width and anteroposterior diameter increase. Increased T1 and T2-weighted signal is noted in both the anterior and posterior pituitary at birth, which decreases in intensity by 6 weeks of age [1].

The posterior pituitary gland demonstrates hyperintensity on T1-weighted and T2-weighted images in 52 and 63% of cases, respectively [2] (Fig. 1). Age-related decline in T1 and T2 signal, as well as physiological variation with stress and dehydration has been demonstrated on MRI. The posterior pituitary hyperintensity is felt to be related to intracellular lipid within the glial pituicytes or neurosecretory granules containing AVP-neurophysin-copeptin complexes. In response to water deprivation, an inverse linear correlation between the signal intensity of the posterior pituitary gland on T1-weighted MR images and plasma vasopressin concentration has been demonstrated.

Clinical presentation

Pathology within the sellar and parasellar region include those involving the pituitary gland, the pituitary stalk (infundibulum) and its surrounding structures. MRI best delineates the mass lesion, determine its epicenter, provide tissue characteristics, and demonstrate potential extension to nearby structures, thereby helping to develop a differential diagnosis and, ultimately, a therapeutic strategy.

Patients with sellar region pathology may be asymptomatic or may present with one of the following categories of symptoms:

(1) Endocrine hyperfunction—Usually due to adenoma producing excess hormones, such as prolactin, adrenocorticotropic hormone (ACTH) or growth hormone, with resultant endocrine syndromes.
(2) Endocrine hypofunction—Usually due to involvement of the pituitary gland, infundibulum or hypothalamus, from the compressive effects of larger lesions on these structures resulting in low secretion of pituitary hormones.
(3) Neurological manifestations related to mass effect—Visual disturbance or other cranial nerve dysfunction, usually related to a large pituitary mass, with supra- or

parasellar extension [3]. Mass effect upon the optic chiasm can result in bitemporal vision loss, while extension into the cavernous sinus may, rarely, result in dysfunction of cranial nerves III, IV, VI or V1 and V2 segments of the trigeminal nerve. Also, rarely, superior extension may lead to mass effect upon the third ventricle, obstructing the latter may result in hydrocephalus. Finally, inferior extension into the sphenoid sinus may result in CSF rhinorrhea, nasopharyngeal obstruction or recurrent sinonasal infections.

(4) Headache—This is an uncommon symptom, which may be related to stretching of the dura, particularly in patients with more aggressive neoplasms.

Sellar and parasellar abnormalities

Pituitary adenomas

Pituitary adenomas constitute the most common intracranial tumors, with an incidence of ~10–17% of the population [4, 5]. In fact, cross-sectional studies in normal volunteers have found small, asymptomatic nonenhancing lesions in the gland in ~10% [6]. Most of these tumors are benign adenomas, with carcinomas constituting only 0.1–0.2%. These typically monoclonal tumors can arise from any cell type within the pituitary gland. Several gene mutations are thought to contribute to the development of pituitary adenomas. Approximately 2.7% of pituitary adenomas are found in the context of MEN-1, whereas, conversely, about 40% of MEN-1 patients have pituitary adenomas. The majority of these secrete prolactin, typically macroadenomas and may be multifocal [3]. Most pituitary adenomas are asymptomatic and found coincidentally on imaging performed for other reasons. In such cases, these abnormalities are often referred to as 'incidentalomas' [5]. Pituitary adenomas become clinically significant only if they are either functional (i.e., produce clinical effects from overproduction of a hormone) or become large enough to extend out of the bony sella into either the suprasellar cistern or the parasellar region.

Pituitary adenomas are classified according to size and function. Based upon size, they are divided into microadenomas (<10 mm), macroadenomas (≥10 mm) or giant adenomas (>40 mm). Functional adenomas constitute approximately two-thirds of cases that present clinically. Prolactinomas are the most common, followed by nonfunctioning adenomas. Other functional types include somatotropinomas (causing acromegaly due to excess secretion of growth hormone), corticotropinomas (causing Cushing's disease due to ACTH overproduction leading to adrenal hyperfunction) and—rarely—thyrotropinomas (causing hyperthyroidism due to excess production of TSH) [4]. After the clinical suspicion is raised, the diagnosis of pituitary hyperfunction is made by biochemical testing for hormonal excess. Adenomas that produce gonadotropins (LH or FSH) are usually inefficient and do not result in a defined clinical syndrome. They thus behave like and are often categorized together with nonfunctional adenomas.

MRI is considered the gold standard for imaging pituitary adenomas by the Congress of Neurological surgeons [7]. MRI is used to assess tumor size, location, extent and whether there is mass effect on surrounding structures (Figs 2 and 3). Microadenoma detection may be significantly impacted by MR sequence selection and the specific contrast administration protocol used. Dynamic, thin section, high-resolution images obtained 1–2 mm apart are optimally obtained through the sellar/parasellar region to look for microadenomas. On MR imaging, the pituitary adenomas vary in appearance from slightly hypointense to isointense on T1-weighted images, like other brain tumors, and from isointense to hyperintense on T2-weighted images [8]. They may also demonstrate intratumoral hemorrhage or internal cystic change.

Suprasellar extension (86%) is more common than sphenoidal extension (35%), based on a study [9] of 220 macroadenomas, with visual field defects seen in 59%. Diagnosis of invasion into the cavernous sinus is suggested once tumor extends below or lateral to the lateral edge of the cavernous internal carotid artery. Encasement of the intracavernous carotid artery is suggested when at least 270 degree of the vessel is surrounded by tumor. Adenomas usually do not cause vessel narrowing as may occur with meningiomas.

Over time, most adenomas tend to be stable in size. Studies with the cell turnover marker Ki-67 show that only about 0.1–3.7% of the cells of a pituitary adenoma divide and contribute to tumor growth. In a systematic review of 11 studies of longitudinal observational cohort studies [10], there was a greater tendency for tumor growth in macroadenomas and solid lesions, as compared with microadenomas and cystic lesions. The overall incidence of new endocrine dysfunction was 2.4 per 100 patient years (PYs)

Nonfunctional adenomas

Nonfunctioning pituitary adenomas (NFPAs) refer to pituitary adenomas which do not demonstrate hypersecretion of pituitary hormones. Natural history studies of NFPAs are few, but growth of 40–50% of untreated asymptomatic NFPAs has been reported in small cohorts of 42 [11] and 28 [12] patients.

Surgery is indicated for symptomatic tumors. Surgical indications for NFPAs, include demonstrated growth on

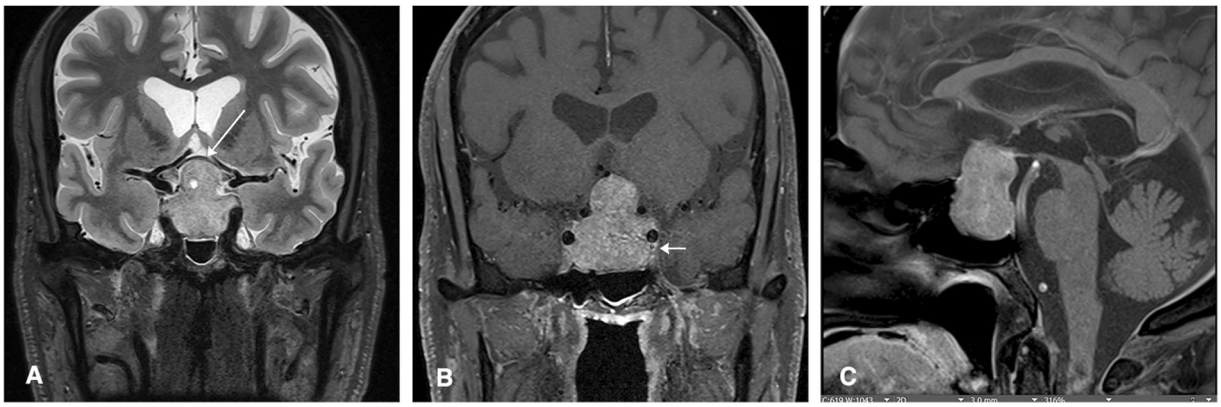

Fig. 2 Macroadenoma: Coronal T2 (**a**) and coronal and sagittal post-contrast T1-weighted images (**b**, **c**) demonstrating a large sellar/suprasellar mass with mass effect upon the optic chiasm (arrow) (**a**) and a snowman appearance (**c**). Parasellar extension into the cavernous sinus (small arrow) is well demonstrated noted on the coronal images

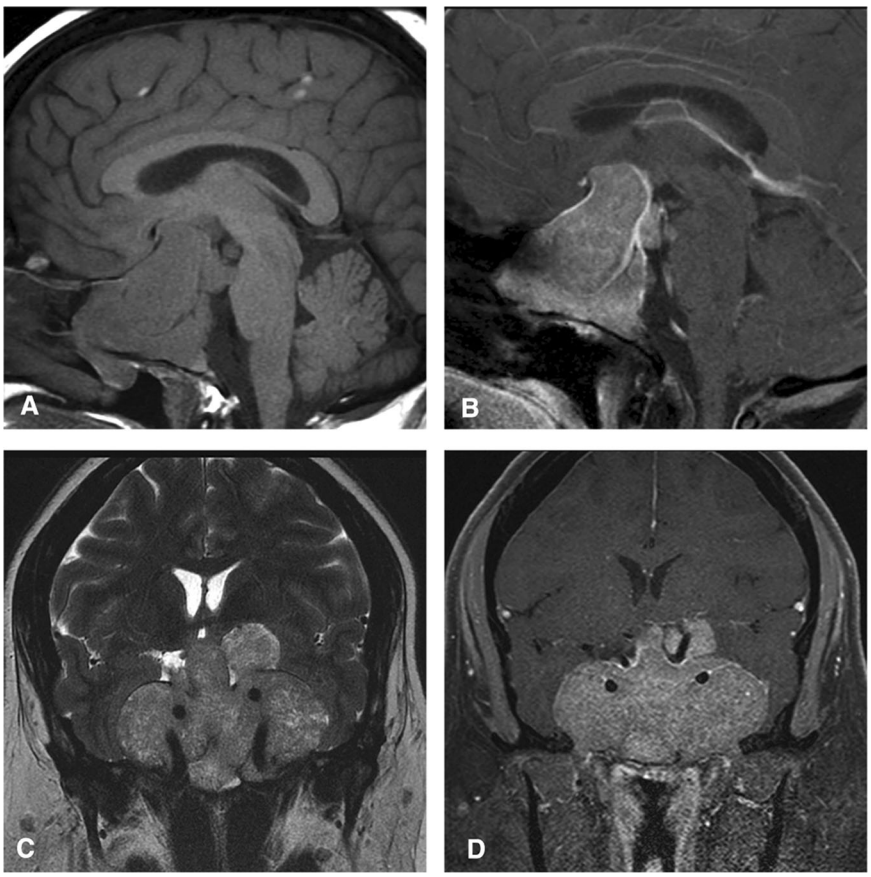

Fig. 3 Giant macroadenoma: Sagittal Pre and Postcontrast T1-weighted images (**a**, **b**) and Coronal T2-weighted (**c**) and postcontrast Coronal T1-weighted image (**d**) demonstrates a large sellar/suprasellar mass producing mass effect upon the hypothalamus superiorly and lateral extension into the cavernous sinuses bilaterally

serial MRI scans, mass effect on the optic chiasm, stalk effect causing hyperprolactinemia, apoplexy, refractory headaches or other neurologic deficits related to compression, and in some circumstances, hypopituitarism [13].

Patients with clinically asymptomatic nonfunctioning adenomas may be followed clinically without specific treatment. Follow up MR exams are used to assess lesions for growth and the timing of future surgery.

MRI may also help surgical planning by showing invasion of surrounding structures that may affect surgical approach. Postoperatively, MRI scans are helpful to document and adequate resection 3 months after surgery [14] and then annually for 3–5 years, and then subsequently less frequently if stable. Postoperative radiotherapy may be indicated for patients with incomplete resection, especially when substantial tumor persists or if there is subsequent growth.

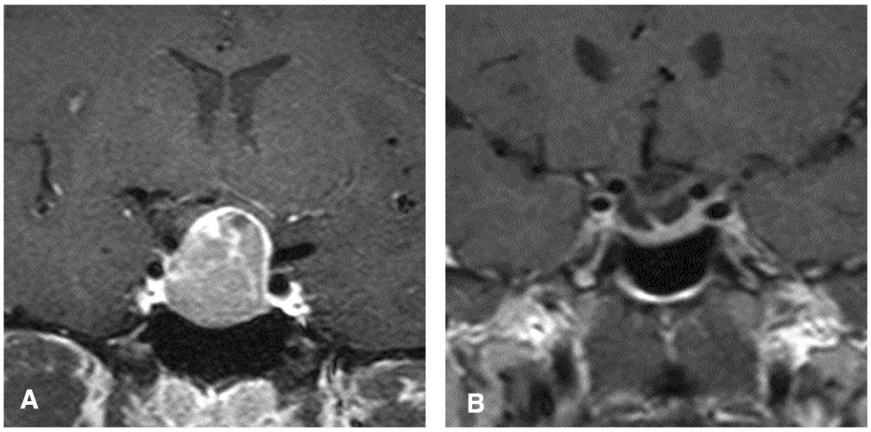

Fig. 4 Response of prolactinoma to medication: Postcontrast T1-weighted MRI demonstrating a large prolactin producing adenoma (**a**) with a significant reduction in size on oral treatment with cabergoline alone (**b**)

Prolactinomas

These constitute ~40–50% of all pituitary tumors. Prior to the age of 50, women exhibit a ten-fold higher frequency of these tumors as compared with men. After age of 50, both genders appear to have equal preponderance [15]. Presentation varies according to size and levels of systemic hormone levels.

The symptom of galactorrhea and/or oligomenorrhea may allow early detection of pituitary prolactinomas in women; therefore, most prolactinomas in women are microadenomas. In contrast, the lack of specific early symptoms (with the exception of the somewhat nonspecific symptom of decreased libido) leads to a later diagnosis in men, who usually present with macroadenomas.

After a biochemical diagnosis is made, confirmation of a pituitary tumor and its extent requires MR imaging. A significant correlation has been found between the tumor size and prolactin levels. Elevations of prolactin level between the upper limit of normal and 100–150 µg/L (2000 mIU/L) can be induced by dopamine antagonist drugs, stalk effect, or functional causes. Above 150 µg/L (3000 mIU/L), prolactin levels are generally due to a prolactinoma. Much higher levels, sometimes into the thousands of µg/L, are typically seen in macroprolactinomas. However, caution is advisable in interpreting results of a prolactin biochemical assay, because dissociation between hormonal levels and tumor size may be present in some individuals [16].

First-line treatment modality for prolactinomas are the dopamine receptor agonist drugs, such as cabergoline and bromocriptine. These are highly effective not only in reducing hormone production and symptoms related to hormonal hyperfunction, but also in causing significant tumor shrinkage and in some patients quick improvement – sometimes within days – of visual field defects [17]. 80–90% patients with microprolactinomas and 70% with macroprolactinomas demonstrate reduction in gland size with medical treatment [16] (Fig. 4).

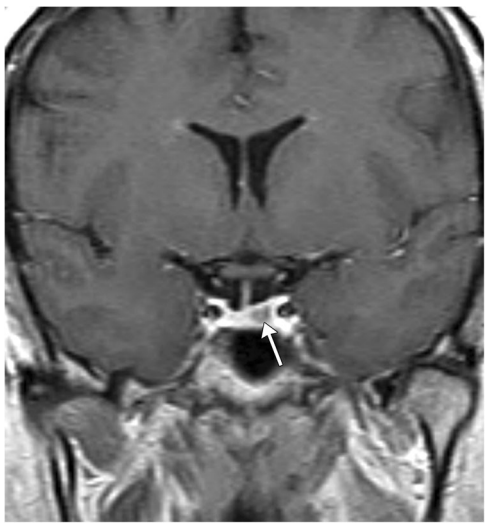

Fig. 5 Cushing's disease: Postcontrast T1-weighted images demonstrate a microadenoma in the left half of the gland in a patient with Cushing's disease

Indications for surgery include intolerance to dopamine agonist therapy, inadequate tumor response to this treatment as evidenced by increasing tumor size or persistent chiasmal compression, pituitary apoplexy, CSF leak during treatment and patient preference. It may also be considered for macroadenomas at risk of encroaching on the optic chiasm in women considering pregnancy [18].

Corticotropinomas

Cushing's disease refers to overproduction of the adrenal hormone cortisol, in response to an ACTH-secreting adenoma of the pituitary gland. ACTH producing adenomas are usually microadenomas (Fig. 5). In fact, only 50% of ACTH-secreting microadenomas are seen on pre and postcontrast T1-weighted sequences [19]. Hence, dynamic postcontrast MRI is imperative to look for these small microadenomas [20]. Surgical resection is considered the

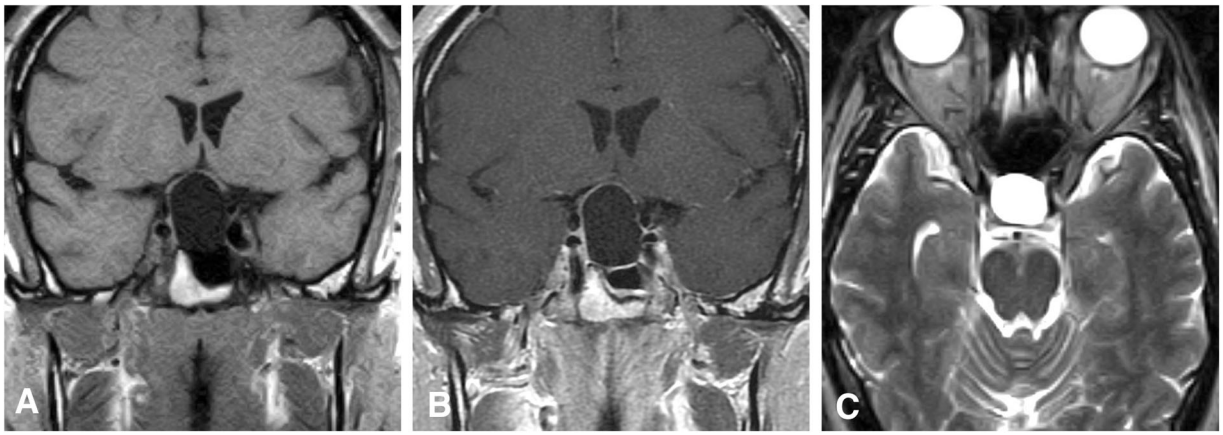

Fig. 6 Rathke's cleft cyst: Noncontrast T1-weighted image (**a**) showing a large sellar/suprasellar mass which demonstrates thin peripheral enhancement on post contrast T1-weighted image and is purely cystic on an axial T2-weighted image (**c**)

treatment of choice for management of Cushing's disease. When there is residual tumor following resection, a variety of medical adrenolytic therapies are available. Ultimately postoperative radiation therapy may be chosen with curative intent. Rarely, bilateral adrenalectomy may need to be considered in refractory cases.

Somatotropinomas

These are responsible for gigantism (in children/teens) and 95% of cases of acromegaly (in adults), with the remainder due to excess GHRH or ectopic GH production by non-pituitary tumors. GH producing adenomas most commonly are either pure somatotroph adenomas, mammosomatotroph adenomas which co-secrete GH and prolactin or mixed tumors [21].

Unlike other adenomas, these are more likely to demonstrate hypointensity on T2-weighted images, in up to 2/3rd of cases [20].

Macroadenomas are detected in up to 77% of subjects [22], with the balance involving microadenomas. If MR scan is unable to identify an offending lesion, consideration should be given to the rare possibility of an extra-pituitary neoplasm producing GH releasing hormone (GHRH) ectopically, usually neuroendocrine neoplasms within the pancreas.

Cystic sellar/parasellar masses

In addition to pituitary adenomas which may become cystic, these include developmental lesions such as Rathke's cleft cysts, craniopharyngiomas, dermoid/epidermoid cysts, colloid cysts or arachnoid cysts [19, 23].

Rathke's cleft cyst

Rathke's cleft cysts are the most common nonneoplastic lesion of the pituitary gland, with an incidence of ~21% by autopsy [24]. Unlike craniopharyngiomas, which are considered neoplastic, Rathke's cleft cysts are considered developmental in origin. They are histologically characterized by the presence of a lining of simple cuboidal or columnar epithelium and contain fluid with a high protein content within it. They are felt to arise from the embryonic remnant of the Rathke's pouch [25], located between the adenohypophysis and the pars intermedia. They are usually purely intrasellar but may extend into the suprasellar region.

They are mostly asymptomatic, but when large, they may become symptomatic. In a review of 118 patients [24, 26] operated for Rathke's cyst, visual impairment or endocrine dysfunction (hormone underproduction) was the most common presenting symptom. Approximately 18% demonstrated recurrence over a 5-year period of follow up after initial resection, suggesting continued growth potential.

They are located intra/suprasellar in 68%, intrasellar in 16%, suprasellar in 13% and intrasphenoidal in 3% [27]. Rathke's cysts are usually in the midline, in or above the anterior portion of the sella turcica and have well-defined margins that are round or lobular. The pituitary stalk and posterior pituitary gland may be displaced posteriorly.

Simple Rathke's cleft cysts are usually homogenous in appearance, whereas more complex cysts are heterogeneous, with regions of wall thickening and contrast enhancement seen in only 3%, which is described as ring-like or capsular. The cyst is iso/hyperintense in 63% and hypointense in 37% on T1-weighted images, while on T2-weighted images, they are hyperintense in 37%, and of variable signal intensity in 63% (Figs 6 and 7). The difference is due to varying protein concentrations of the cyst contents. Calcification is not seen in Rathke's cleft cysts (as opposed to craniopharyngiomas), although exceptions have been reported. A nonenhancing T1-hyperintense and T2-hypointense intracystic nodule is felt to be characteristic of Rathke's cleft cysts.

These nonneoplastic lesions are usually stable but may have a slow growth rate. Follow-up imaging is performed to

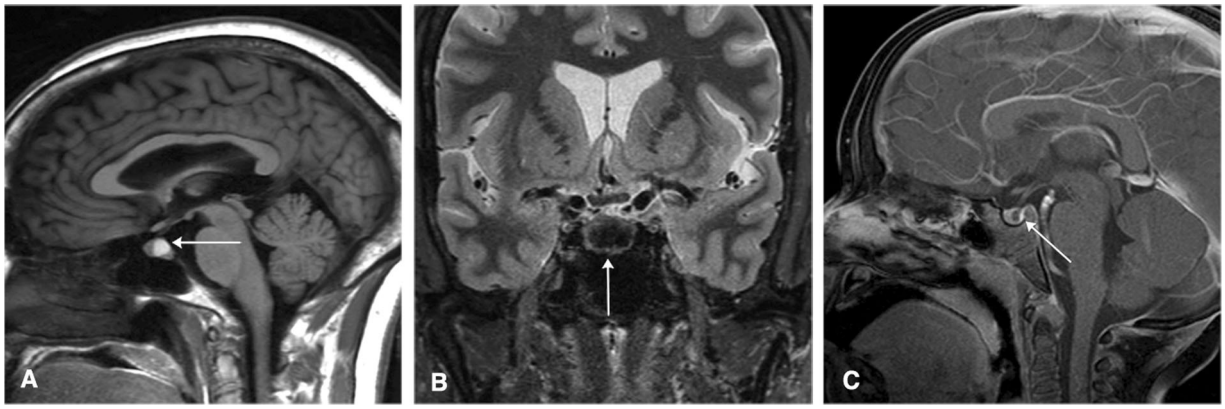

Fig. 7 Rathke's cleft cyst: Sagittal noncontrast T1-weighted image demonstrates a T1-hyperintense lesion (A-arrow) between the anterior and posterior pituitary lobes which is hypointense on T2-weighted image (B-arrow) and does not enhance on the postcontrast image (C-arrow)

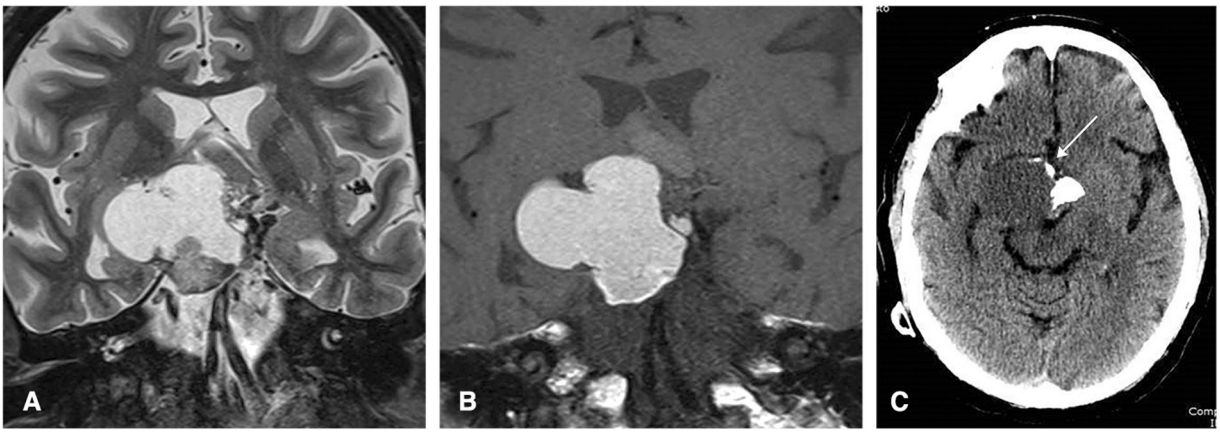

Fig. 8 Craniopharyngioma: T2-weighted image (**a**) demonstrates a large suprasellar cystic mass which is T1-hyperintense on noncontrast MRI images reflecting an increased protein content. CT images reveal the calcified rim (arrow) typical of craniopharyngiomas (Unlike Rathke's cleft cysts)

ensure lack of growth over time [28]. A suprasellar cyst location, occurrence of squamous metaplasia, and isointensity on T2-weighted MRI were independent predictors of Rathke's cleft cyst recurrence.

Craniopharyngioma

Craniopharyngiomas are solid or mixed solid-cystic benign tumors, which are predominantly suprasellar in location but may extend into the sella. They are thought to arise from ectodermal cell rests in the anterior pituitary stalk, usually at the transition with the pars distalis.

About 50% present clinically during childhood and adolescence, while the other 50% present after age 20, though some not until age 70 or 80. Histologically, most of craniopharyngiomas are adamantinomatous, while the papillary form is more common in the elderly.

On imaging, these usually appear as a mixed solid/cystic mass, with areas of enhancement and calcification within its walls (Fig. 8). The papillary form usually appears solid and calcifies only rarely [29, 30]. Approximately 20% have intrasellar extension, although 4–6% may be purely intrasellar. Almost all, 94% of these, have an extrasellar component [31], with extension into the anterior, middle or posterior cranial fossae.

Craniopharyngiomas demonstrate growth over time on sequential MR exams, if untreated [31] and may be locally destructive. As a result, they are commonly associated with pituitary hormone deficiencies, including diabetes insipidus. They are usually treated by surgical resection, especially if they produce symptoms or demonstrate growth [32]. Surgery is often difficult due to the location and tenacity of these tumors. Radiotherapy is usually reserved for patients with residual/recurrent tumors.

Arachnoid cyst

These can rarely involved the sella and are either congenital or acquired. They are related to herniation of the basal arachnoid membrane through an incomplete diaphragma

sellae [23, 33]. They are usually seen as smooth-walled cystic lesions without enhancement of the internal contents or its wall after contrast administration (Fig. 9).

Pituitary stalk lesions

The pituitary stalk or infundibulum is a critical part of the hypothalamic-pituitary axis. Its integrity is crucial for the normal functioning of the pituitary gland since it is responsible for delivering signaling factors from the hypothalamus to the pituitary. Any pathology involving the infundibulum can, therefore, have profound systemic effects. A short list of pathologies is shown in Table 1.

Given the critical location of these lesions, these are rarely biopsied and diagnosis often rests on ancillary findings.

Clinical features

These conditions usually present clinically with central diabetes insipidus (DI), characterized by polydipsia and polyuria related to abnormal/decreased vasopressin (ADH) secretion. Anterior pituitary hormone deficits may also be demonstrated.

Imaging

Loss of hyperintense signal of the posterior pituitary has been described as the most specific imaging sign in the diagnosis of central DI [34]. However, the more important role of imaging in patients with central DI is to assess a specific cause, such as those in the table which will result in a mass in or enlargement of the pituitary stalk (Fig. 10). While various different patterns of stalk enhancement (e.g., uniform vs rounded) have been described to differentiate inflammatory from neoplastic disorders, there is a substantial overlap between these groups [35]. The differential diagnosis for thickening and mass-like enlargement of the pituitary stalk includes Langerhans-cell granulomatosis in very young children, germ-cell tumors in adolescents, while sarcoidosis should be considered in older individuals. MRI follow up in 3–6 months should be considered in patients who are otherwise asymptomatic to ensure stability.

Miscellaneous abnormalities

Hypophysitis/ Infundibuloneurohypophysitis

This refers to an inflammatory process involving either the anterior pituitary (Lymphocytic adenohypophysitis or LAH), the infundibulum and neurohypophysis (Lymphocytic infundibuloneurohypophysitis or LINH) or both (Lymphocytic panhypophysitis or LPH) [36–38]. These disorders typically affect young and middle-aged women (male:female ratio, 1:6), although they have been described in both younger and elderly patients. IgG-4 related hypophysitis has also been described, although predominantly affecting men (2.4:1) [39, 40]. More recently, hypophysitis

Table 1 Causes of infundibular pathology

Congenital	Hypoplasia, duplication
Inflammatory	Sarcoidosis
	Langerhans-cell histiocytosis
	Tuberculosis
	Wegener's disease
	Whipple's disease
	Infundibuloneurohypophysitis
	Erdheim–Chester disease
Neoplastic	Metastases (Breast, Lung cancers, others)
	Lymphoma/Leukemia
	Germ-cell tumors
	Pituitary adenoma
	Pituicytoma/Tanycytoma
	Granular cell tumors

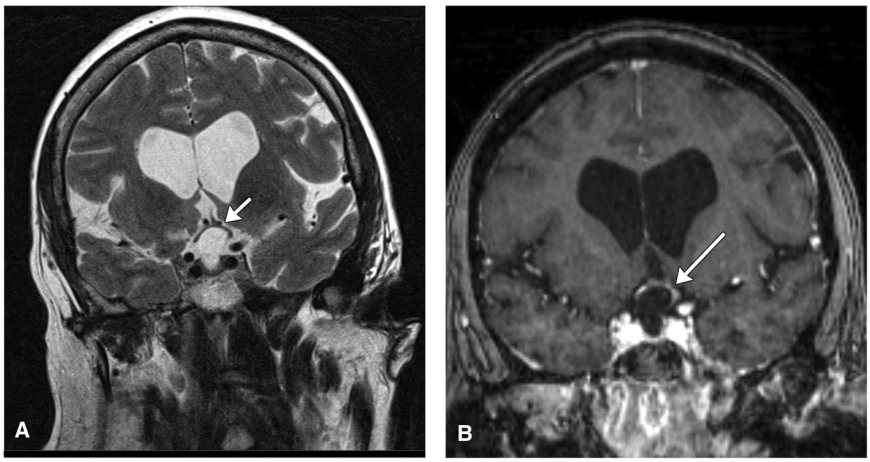

Fig. 9 Arachnoid Cyst: T2-weighted coronal (**a**) and postcontrast T1-weighted coronal image (**b**) reveals a cystic lesion within the sella extending into the suprasellar region causing mass effect on the inferior aspect of the optic chiasm (arrow). Postcontrast image reveals the nonenhancing nature of the cyst with a leftward displaced **pituitary gland** and infundibulum (thick arrow)

Fig. 10 Infundibular pathology: Postcontrast T1-weighted image reveals a thickened pituitary infundibulum (arrow) and (**a**) multiple air containing cystic spaces within the lung parenchyma on a chest CT (**b**) in a patient with Langerhans-cell histiocytosis

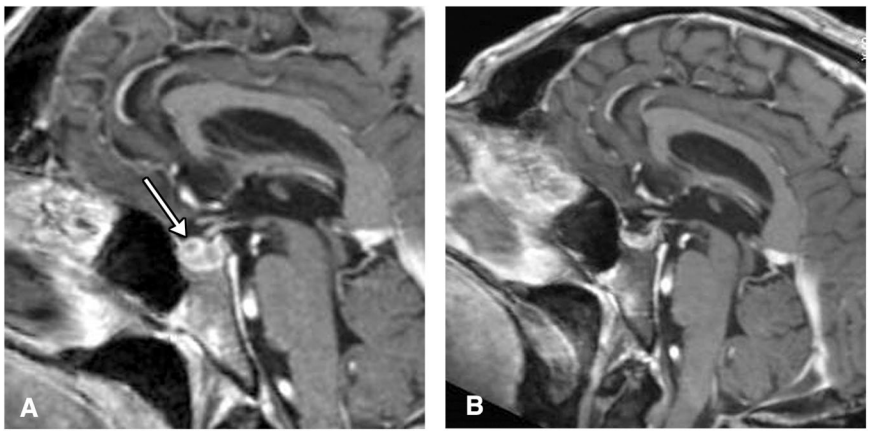

Fig. 11 Hypophysitis**:** Postcontrast T1-weighted MR images demonstrating an enlarged anterior pituitary gland (arrow) (**a**) with shrinkage on steroid usage (**b**)

is being seen with increased frequency as an endocrine adverse event from check-point inhibitor immune therapy for a variety of cancers [41] (see below).

Histologically, three main pathological subtypes have been described—lymphocytic, granulomatous and xanthomatous. The lymphocytic subtype is the most common, with other rarer ones consisting of the necrotizing, IgG4 plasmacytic and mixed forms. These are believed to be autoimmune mediated, as evidenced by presence of autoantibodies to arginine-vasopressin (AVP) secreting cells. Pathologically, they are characterized by the presence of chronic inflammatory changes with plasma cell and lymphocytic infiltration.

Clinically, partial or panhypopituitarism occurs in 80% of patients with hypophysitis [37, 38], central diabetes insipidus in 15%, or symptoms related to a pituitary mass effect (such as headaches or visual disturbances) in 40–60%.

On imaging, there is a variable degree of mass-like thickening of the pituitary infundibulum and the adenohypophysis (Fig. 11).

Treatment is predominantly symptomatic. Steroids may result in clinical and radiological improvement in some patients. MR follow up is again helpful to ensure resolution.

With the recent proliferation of immune-checkpoint inhibitor therapy (ipilimumab, nivolumab [42] and pembrolizumab) for various solid cancers, there has been an increased presentation of patients with hypophysitis. These drugs enhance T-cell activation that not only produces an anti-neoplastic effect, but also multiple endocrine abnormalities, including hypophysitis, primary hyper- and hypothyroidism and primary adrenal insufficiency. Ipilimumab is a monoclonal antibody that blocks cytotoxic T-lymphocyte antigen-4 (CTLA-4), an inhibitory molecule expressed on antigen-stimulated T cells, while nivolumab is a monoclonal antibody directed against the programmed cell death-1 (PD-1) receptor. The antigenic target in the pituitary gland has not been identified. In a cohort of patients receiving ipilimumab for metastatic melanoma, immune therapy induced hypophysitis (IH) was diagnosed in 17 of 154 patients (11.0%) [41], of which 15 were male, unlike autoimmune hypophysitis which is predominately a disease of women. Headache was the most common symptom (14/17), others being fatigue (10/17), nausea, decreased appetite, cold intolerance, hot flashes, weight loss, dizziness, blurry vision and confusion. All patients with immune hypophysitis developed anterior hypopituitarism.

MRI demonstrated mild to moderate, diffuse pituitary enlargement with variable enhancement after contrast administration in all patients with immune hypophysitis, with

stalk thickening seen in 10/17. The pituitary enlargement preceded the clinical diagnosis of hypophysitis in eight patients, often by several weeks, while two of these patients were asymptomatic at the time of imaging. Treatment is supportive and usually involves holding immune therapy and treatment with high-dose glucocorticoids. Radiographic resolution of pituitary enlargement was observed in most patients (15/17), although hypopituitarism persisted in most patients (13/17). Reversal of imaging changes occurred rapidly and was observed in all patients who underwent repeat imaging within 40 days of the diagnosis.

Pituitary hemorrhage/apoplexy

Pituitary apoplexy refers to a sometimes dramatic clinical syndrome characterized by hemorrhage and/or infarction within the pituitary gland, usually within a pituitary adenoma [43]. This is characterized by sudden enlargement of the gland with acute headache, pituitary insufficiency and visual abnormalities either from chiasm or cavernous sinus compression. Subclinical (asymptomatic) intratumoral hemorrhage is much more frequent than acute apoplexy, with up to 25% of all pituitary tumors displaying hemorrhagic and/or necrotic areas either on imaging or at autopsy. In a systematic review [10], there was a greater incidence of pituitary apoplexy and new endocrine dysfunction in macroadenomas compared with microadenomas, with an overall prevalence of 0.6% and an incidence of 0.17 per 100,000 person-year [44].

MR is helpful in the detection of pituitary hemorrhage. Acute hemorrhage is usually seen as T1 hypointense and hyperintense on T2-weighted images [45]. On the other hand, subacute hemorrhage may appear hyperintense on T1-weighted sequences and may be indistinguishable from T1 hyperintense Rathke's cleft cysts with a high protein content. Follow up over time or comparison with prior imaging may be considered in these cases to assess for evolution of hemorrhage over time, as opposed to a Rathke's cleft cyst which would normally maintain a T1-hyperintense signal.

Pituitary hemorrhage had been considered a neurosurgical emergency in the past, but reports of spontaneous clinical recovery and/or tumor resolution have engendered the adoption of a conservative approach in selected cases [43]. Urgent neurosurgical intervention may be considered if there is mass effect on surrounding structures, otherwise conservative management with follow up MRI in 2–3 months may be considered in stable patients, with replacement of relevant pituitary hormone deficits.

Pituitary hyperplasia

Pituitary hyperplasia refers to diffuse enlargement of the pituitary gland without demonstrable nonenhancing areas. This may be reported as a sellar mass and be misdiagnosed as a pituitary adenoma or infiltrative disease. Occasionally, the pituitary gland may become large enough to extend into suprasellar cistern or even occasionally abut the optic chiasm. Causes include:

(1) Pregnancy and postpartum—related to lactotroph hyperplasia
(2) Long-standing untreated primary hypothyroidism and primary hypogonadism—related to thyrotroph and gonadotroph hyperplasia, respectively
(3) Puberty—due to somatotroph hyperplasia
(4) Nelson syndrome—from corticotroph hyperplasia following bilateral adrenal resection

Parasellar masses

The pituitary gland and function may also be affected by mass effect from a myriad of parasellar masses arising from surrounding structures which may produce stalk effect or hypopituitarism. These include but are not limited to meningiomas (Fig. 12), germ-cell tumor (Fig. 13), lymphoma, plasmacytoma, metastases etc. Follow up is usually determined by the degree of neoplastic grade of tumor and

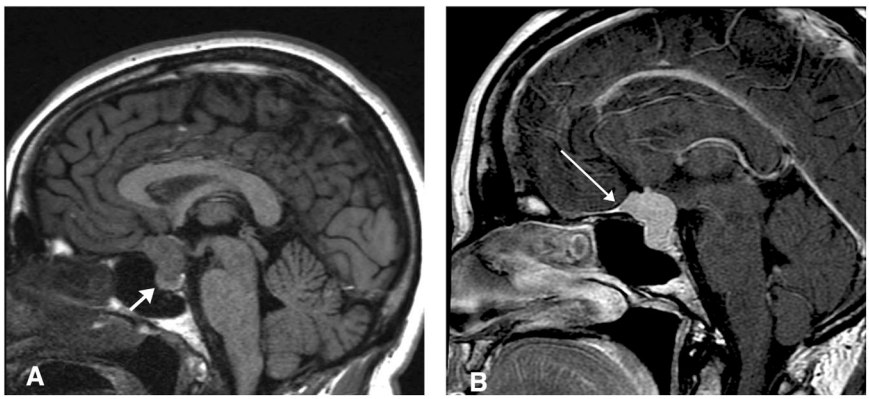

Fig. 12 Meningioma: Sagittal precontrast T1 (**a**) and postcontrast (**b**) T1-weighted images reveal a diffusely enhancing predominantly suprasellar mass with a dural tail (arrow) arising from the tuberculum sella. The normal pituitary gland is better seen on the noncontrast image (arrow in a), inferiorly displaced due to mass effect from above

interval surgical management, with more frequent follow up for more malignant etiologies like lymphoma and germinomas.

Sellar aneurysm

This is an important entity which needs to be differentiated from other sellar masses, considering the grave consequences of inadvertent surgery. These can arise from the internal carotid or anterior cerebral arteries [19]. MRI can help in the differential diagnosis by demonstrating the presence of markedly hypointense flow voids within the lesion. MR/CT angiography may be diagnostic by demonstrating the enlarged lumen of the aneurysm (Fig. 14).

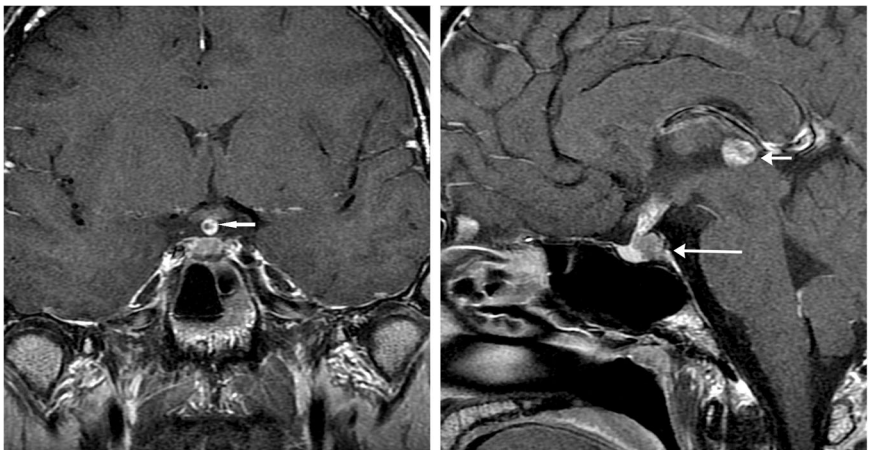

Fig. 13 Germ-cell tumor: Postcontrast coronal (**a**) and sagittal (**b**) T1-weighted image in a 23 year old male patient, demonstrates a thickened pituitary infundibulum in image A (arrow), mass-like appearance of the posterior pituitary gland (long arrow). Also seen is a mass in the pineal gland (small arrow)

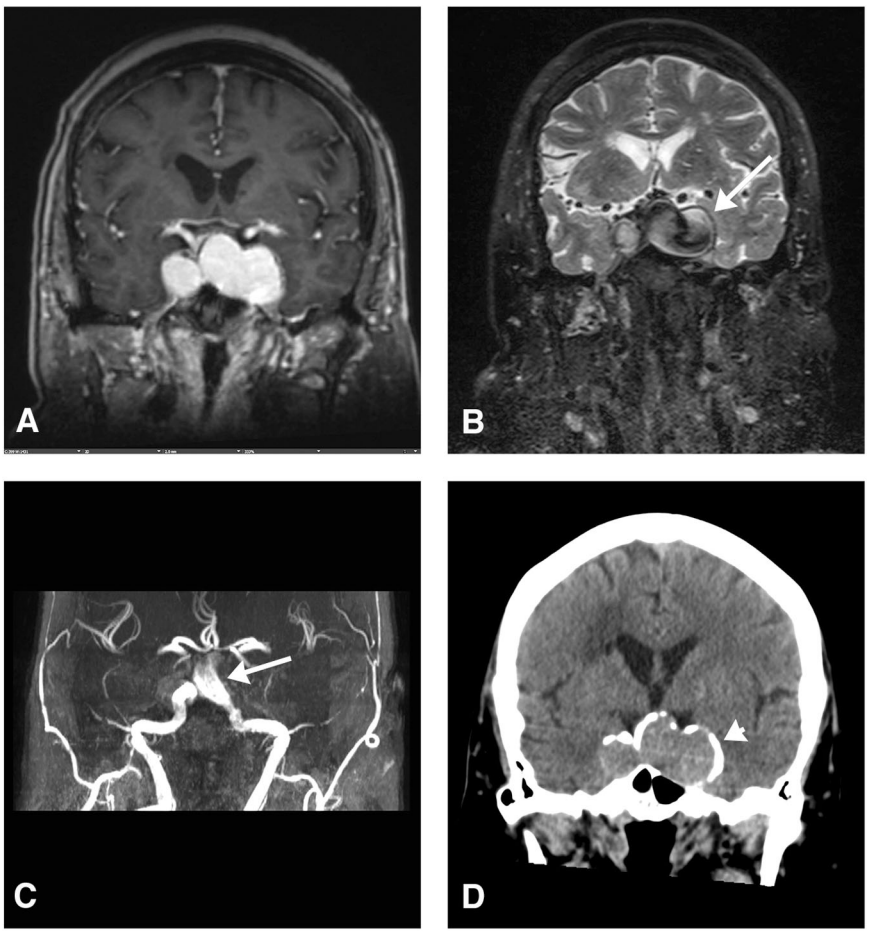

Fig. 14 Sellar aneurysms: Postcontrast T1-weighted image (**a**) reveals large sellar and bilateral parasellar masses resembling large macroadenomas. T2-weighted image (**b**), however reveals large markedly hypointense flow voids within the masses (arrow). MR angiographic image (**c**) reveals the dilated lumen of the cavernous segments of both carotid arteries. A coronal noncontrast CT image (**d**) demonstrates peripheral calcifications (arrowhead) surrounding these large bilateral cavernous ICA aneurysms

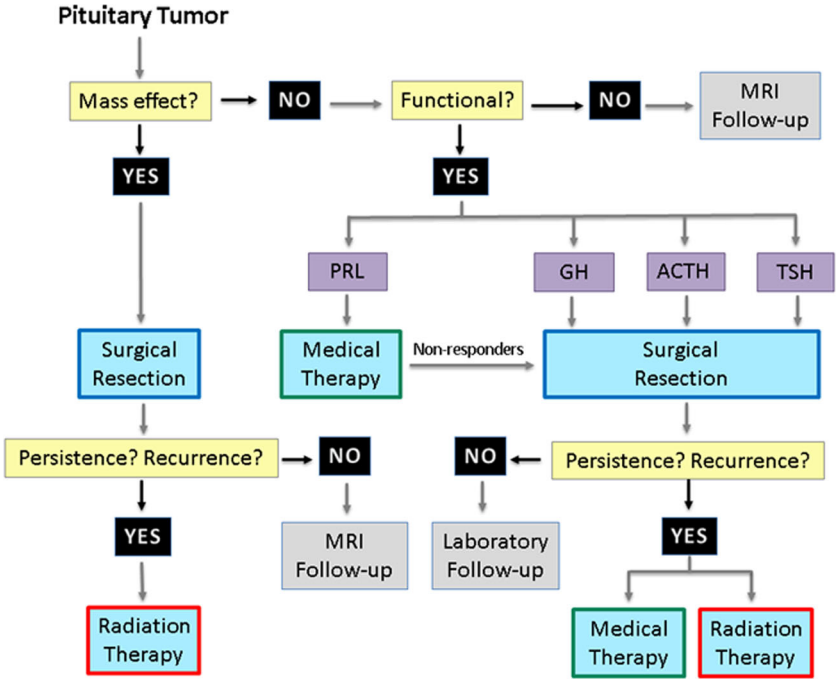

Fig. 15 Algorithm showing proposed decision branch points for the management of pituitary tumors. Major branch points are shown in yellow, and separate pituitary lesions are based on the presence of mass effect, hormone secretion, and response to treatment. Treatment is shown in blue, with surgical, medical, or radiotherapy management outlined in blue, green, and red, respectively. Tracking the course of therapy is shown in gray, and includes following the lesion for changes in size on MRI and trending hormone levels

Algorithm for assessment and management of pituitary pathology

In Fig. 15, we propose an algorithm describing the evaluation and management of pituitary tumors. The best workup will involve careful collaboration between multiple specialties, including endocrinology, neurosurgery, neuro-ophthalmology, radiation oncology and neuroradiology.

Conclusion

MRI plays a central role in the diagnosis and current management of pituitary tumors. It is used to diagnose sellar and parasellar pathology in patients with suspect symptoms. Once diagnosed, MR is central to direct management of pituitary lesions – larger tumors causing mass effect upon surrounding significant structures often require surgery, while the smaller lesions may benefit from medical management. MR is also essential in the follow up of diagnosed and treated tumors to assess response to therapy and thereby direct secondary treatment options.

Compliance with ethical standards

Conflict of interest The authors declare that they have no conflict of interest.

Publisher's note Springer Nature remains neutral with regard to jurisdictional claims in published maps and institutional affiliations.

References

1. R.B. Dietrich, L.E. Lis, F.S. Greensite, D. Pitt, Normal MR appearance of the pituitary gland in the first 2 years of life. Am. J. Neuroradiol. **16**, 1413–1419 (1995)
2. B.S. Brooks, T. el Gammal, J.D. Allison, W.H. Hoffman, Frequency and variation of the posterior pituitary bright signal on MR images. Am. J. Neuroradiol. **10**, 943–948 (1989)
3. R.R. Lleva, S.E. Inzucchi, Diagnosis and management of pituitary adenomas. Curr. Opin. Oncol. **23**, 53–60 (2011)
4. M.E. Molitch, Diagnosis and treatment of pituitary adenomas: a review. Jama **317**, 516–524 (2017)
5. M.E. Molitch, Pituitary incidentalomas. Best. Pract. Res. Clin. Endocrinol. Metab. **23**, 667–675 (2009)
6. W.A. Hall, M.G. Luciano, J.L. Doppman, N.J. Patronas, E.H. Oldfield, Pituitary magnetic resonance imaging in normal human volunteers: occult adenomas in the general population. Ann. Intern Med **120**, 817–820 (1994)
7. C.C. Chen, B.S. Carter, R. Wang, K.S. Patel, C. Hess, M.E. Bodach et al. Congress of neurological surgeons systematic review and evidence-based guideline on preoperative imaging assessment of patients with suspected nonfunctioning pituitary adenomas. Neurosurgery **79**, E524–E526 (2016)
8. A. Hagiwara, Y. Inoue, K. Wakasa, T. Haba, T. Tashiro, T. Miyamoto, Comparison of growth hormone-producing and non-growth hormone-producing pituitary adenomas: imaging characteristics and pathologic correlation. Radiology **228**, 533–538 (2003)
9. J. Gsponer, N. De Tribolet, J.P. Deruaz, R. Janzer, A. Uske, R.O. Mirimanoff et al. Diagnosis, treatment, and outcome of pituitary tumors and other abnormal intrasellar masses. Retrospective analysis of 353 patients. Med. (Baltim.) **78**, 236–269 (1999)
10. M.M. Fernandez-Balsells, M.H. Murad, A. Barwise, J.F. Gallegos-Orozco, A. Paul, M.A. Lane et al. Natural history of non-functioning pituitary adenomas and incidentalomas: a systematic review and metaanalysis. J. Clin. Endocrinol. Metab. **96**, 905–912 (2011)

11. K. Arita, A. Tominaga, K. Sugiyama, K. Eguchi, K. Iida, M. Sumida et al. Natural course of incidentally found nonfunctioning pituitary adenoma, with special reference to pituitary apoplexy during follow-up examination. J. Neurosurg. **104**, 884–891 (2006)
12. O.M. Dekkers, S. Hammer, R.J. de Keizer, F. Roelfsema, P.J. Schutte, J.W. Smit et al. The natural course of non-functioning pituitary macroadenomas. Eur. J. Endocrinol. **156**, 217–224 (2007)
13. J.W. Lucas, M.E. Bodach, L.M. Tumialan, N.M. Oyesiku, C.G. Patil, Z. Litvack et al. Congress of neurological surgeons systematic review and evidence-based guideline on primary management of patients with nonfunctioning pituitary adenomas. Neurosurgery **79**, E533–E535 (2016)
14. P.J. Yeh, J.W. Chen, Pituitary tumors: surgical and medical management. Surg. Oncol. **6**, 67–92 (1997)
15. T. Mancini, F.F. Casanueva, A. Giustina, Hyperprolactinemia and prolactinomas. Endocrinol. Metab. Clin. North Am. **37**, 67–99 (2008). viii
16. F.F. Casanueva, M.E. Molitch, J.A. Schlechte, R. Abs, V. Bonert, M.D. Bronstein et al. Guidelines of the Pituitary Society for the diagnosis and management of prolactinomas. Clin. Endocrinol. (Oxf.) **65**, 265–273 (2006)
17. M.E. Molitch, Medical treatment of prolactinomas. Endocrinol. Metab. Clin. North Am. **28**, 143–169 (1999). vii
18. A. Klibanski, Clinical practice. Prolactinomas. N. Engl. J. Med **362**, 1219–1226 (2010)
19. M. Buchfelder, S. Schlaffer, Imaging of pituitary pathology. Handb. Clin. Neurol. **124**, 151–166 (2014)
20. J.F. Bonneville, F. Bonneville, F. Cattin, Magnetic resonance imaging of pituitary adenomas. Eur. Radio. **15**, 543–548 (2005)
21. L. Katznelson, E.R. Laws Jr, S. Melmed, M.E. Molitch, M.H. Murad, A. Utz et al. Acromegaly: an endocrine society clinical practice guideline. J. Clin. Endocrinol. Metab. **99**, 3933–3951 (2014)
22. A. Mestron, S.M. Webb, R. Astorga, P. Benito, M. Catala, S. Gaztambide et al. Epidemiology, clinical characteristics, outcome, morbidity and mortality in acromegaly based on the Spanish Acromegaly Registry (Registro Espanol de Acromegalia, REA). Eur. J. Endocrinol. **151**, 439–446 (2004)
23. J.L. Shin, S.L. Asa, L.J. Woodhouse, H.S. Smyth, S. Ezzat, Cystic lesions of the pituitary: clinicopathological features distinguishing craniopharyngioma, Rathke's cleft cyst, and arachnoid cyst. J. Clin. Endocrinol. Metab. **84**, 3972–3982 (1999)
24. A. Teramoto, K. Hirakawa, N. Sanno, Y. Osamura, Incidental pituitary lesions in 1,000 unselected autopsy specimens. Radiology **193**, 161–164 (1994)
25. S.Q. Wolfe, R.C. Heros, Editorial. J. Neurosurg. **112**, 1322–1323 (2010)
26. C.J. Aho, C. Liu, V. Zelman, W.T. Couldwell, M.H. Weiss, Surgical outcomes in 118 patients with Rathke cleft cysts. J. Neurosurg. **102**, 189–193 (2005)
27. L. Cervoni, M. Artico, M. Salvati, S. Carloia, Rathke's cleft cyst: a clinical and radiographic review. Ital. J. Neurol. Sci. **18**, 37–40 (1997)
28. S. Chotai, Y. Liu, J. Pan, S. Qi, Characteristics of Rathke's cleft cyst based on cyst location with a primary focus on recurrence after resection. J. Neurosurg. **122**, 1380–1389 (2015)
29. S.M. Tavangar, B. Larijani, A. Mahta, S.M. Hosseini, M. Mehrazine, F. Bandarian, Craniopharyngioma: a clinicopathological study of 141 cases. Endocr. Pathol. **15**, 339–344 (2004). Winter
30. T.B. Crotty, B.W. Scheithauer, W.F. Young Jr, D.H. Davis, E.G. Shaw, G.M. Miller et al. Papillary craniopharyngioma: a clinicopathological study of 48 cases. J. Neurosurg. **83**, 206–214 (1995)
31. N. Karavitaki, C. Brufani, J.T. Warner, C.B. Adams, P. Richards, O. Ansorge et al. Craniopharyngiomas in children and adults: systematic analysis of 121 cases with long-term follow-up. Clin. Endocrinol. (Oxf.) **62**, 397–409 (2005)
32. R. Sorva, O. Heiskanen, Craniopharyngioma in Finland. Acta Neurochirurgica **81**, 85–89 (1986)
33. M. Güdük, M. HamitAytar, A. Sav, Z. Berkman, Intrasellar arachnoid cyst: a case report and review of the literature. Int. J. Surg. case Rep. **23**, 105–108 (2016)
34. F. Gudinchet, F. Brunelle, M.O. Barth, V. Taviere, R. Brauner, R. Rappaport et al. MR imaging of the posterior hypophysis in children. AJR Am. J. Roentgenol. **153**, 351–354 (1989)
35. A.F. Turcu, B.J. Erickson, E. Lin, S. Guadalix, K. Schwartz, B.W. Scheithauer et al. Pituitary stalk lesions: the Mayo Clinic experience. J. Clin. Endocrinol. Metab. **98**, 1812–1818 (2013)
36. B.E. Hamilton, K.L. Salzman, A.G. Osborn, Anatomic and pathologic spectrum of pituitary infundibulum lesions. AJR Am. J. Roentgenol. **188**, W223–W232 (2007)
37. M.E. Molitch, M.P. Gillam, Lymphocytic hypophysitis. Horm. Res **68**, 145–150 (2007)
38. P. Caturegli, C. Newschaffer, A. Olivi, M.G. Pomper, P.C. Burger, N.R. Rose, Autoimmune hypophysitis. Endocr. Rev. **26**, 599–614 (2005)
39. H. Bando, G. Iguchi, H. Fukuoka, M. Taniguchi, M. Yamamoto, R. Matsumoto et al. The prevalence of IgG4-related hypophysitis in 170 consecutive patients with hypopituitarism and/or central diabetes insipidus and review of the literature. Eur. J. Endocrinol. **170**, 161–172 (2014)
40. J. Shikuma, K. Kan, R. Ito, K. Hara, H. Sakai, T. Miwa et al. Critical review of IgG4-related hypophysitis. Pituitary **20**, 282–291 (2017)
41. M.N. Joshi, B.C. Whitelaw, M.T. Palomar, Y. Wu, P.V. Carroll, Immune checkpoint inhibitor-related hypophysitis and endocrine dysfunction: clinical review. Clin. Endocrinol. (Oxf.) **85**, 331–339 (2016)
42. Y. Okano, T. Satoh, K. Horiguchi, M. Toyoda, A. Osaki, S. Matsumoto et al. Nivolumab-induced hypophysitis in a patient with advanced malignant melanoma. Endocr. J. **63**, 905–912 (2016)
43. C. Briet, S. Salenave, J.-F. Bonneville, E.R. Laws, P. Chanson, Pituitary apoplexy. Endocr. Rev. **36**, 622–645 (2015)
44. A. Raappana, J. Koivukangas, T. Ebeling, T. Pirila, Incidence of pituitary adenomas in Northern Finland in 1992–2007. J. Clin. Endocrinol. Metab. **95**, 4268–4275 (2010)
45. N. Kurihara, S. Takahashi, S. Higano, H. Ikeda, S. Mugikura, L. N. Singh et al. Hemorrhage in pituitary adenoma: correlation of MR imaging with operative findings. Eur. Radiol. **8**, 971–976 (1998)